Annales Geophysicae (2002) 20: 2039–2045

Annales Geophysicae

Effects of temperature dependence of reaction N_2 ($A^3\sum_u^+$)+ O on greenline dayglow emission

A. K. Upadhayaya and V. Singh

Department of Physics, IIT Roorkee 247667, India

Received: 7 February 2002 – Revised: 3 July 2002 – Accepted: 4 July 2002

Abstract. The greenline dayglow emission profiles measured by the Wind Imaging Interferometer (WINDII) on the Upper Atmosphere Research Satellite (UARS) are modelled using recently proposed revisions to the temperature dependent rate coefficient of the reaction N_2 ($A^3\sum_u^+$)+ O in the glow model. The volume emission rates of greenline dayglow emissions are calculated using the Hinteregger et al. (1981) and Tobiska (1991) solar flux models. It is found that the average modelled profiles obtained using the Hinteregger et al. (1981) solar flux model with the temperature dependent rate coefficient and a quantum yield of 0.36 for the reaction N_2 ($A^3\sum_u^+$)+ O agree to within 8% of the observed profiles in the thermospheric peak region, which shows significant improvement over the earlier results (20% smaller than WINDII results) obtained using the temperature independent reaction rate coefficient. On the other hand, the average modelled profiles obtained with a temperature dependent rate coefficient in the Tobiska (1991) solar flux model are about 12% higher than the WINDII results, whereas with the temperature independent rate coefficient the results are about 10% smaller than the WINDII results in the thermospheric peak region. The present study reveals that the emission profiles obtained using the Hinteregger et al. (1981) solar flux model, along with the temperature dependent rate coefficient and a quantum yield of 0.36 for the reaction N_2 ($A^3\sum_u^+$)+ O in glow model, reproduce the thermospheric emission peak as observed by WINDII, a capability which eluded earlier models. These findings support the newly discovered temperature dependence of the rate coefficient of reaction N_2 ($A^3\sum_u^+$) with O.

Key words. Ionosphere (ionization mechanisms; modeling and forecasting; general or miscellaneous)

1 Introduction

In recent years, a number of studies have been done to examine the greenline dayglow emission (Wittase et al., 1999; Singh and Tyagi, 1997; Singh et al., 1996; Torr et al., 1993; Bates 1990; Akmaev and Shved, 1980; Frederick et al., 1976; Feldman et al., 1971; Wallace and Mc Elory, 1966). These studies have given the theoretical models, as well as the experimental data for this important atomic oxygen emission at 5577 Å. Though the theoretical models have taken into account all the well-known sources of greenline dayglow emission, along with the latest atmospheric parameters such as collision cross sections, reaction rate coefficients and quantum yields, these models are still unable to explain the measurements. These models need further refinement so that a better agreement may be achieved between the model results and the experimental observations. Further, the global measurements of dayglow greenline are needed for comparison purposes. The available database on the greenline dayglow emission has recently been expanded as a result of observations made with the Wind Imaging Interferometer (WINDII) on board the Upper Atmosphere Research Satellite (Shepherd et al., 1993). In the thermospheric emission peak region, photoelectron impact excitation of O, dissociative recombination of O_2^+ and the reaction of N_2 ($A^3\sum_u^+$) with O are the major sources of O(^{1}S). The cross sections, quantum yields and reaction rate coefficients for the first two processes have been found consistent with the dayglow emissions. On the other hand, the quantum yield of O(^{1}S) production due to the reaction N_2 ($A^3\sum_u^+$) with O has been the subject of considerable discussion in the literature (Frederick et al., 1976; Torr et al., 1993; Bucsela et al., 1998). In their analysis, Singh et al. (1996) and Tyagi and Singh (1998) used the value of 0.36 for the quantum yield, since it gave the best global fit to all of the measured profiles. However, with this value the model was found to underestimate the measured profiles in the majority of the cases in the thermospheric emission peak region.

In the model calculations of Singh et al. (1996) and Tyagi and Singh (1998), the reaction rate coefficient for the reaction N_2($A^3\sum_u^+$) + O was used from Piper et al. (1981). Recently, Hill et al. (2000) have proposed revisions to this rate coefficient based on their analysis of middle-ultraviolet (MUV) measurements from the rocket-borne MUSTANG spectrometer and the shuttle-borne GLO spectrometer. The major

Correspondence to: V. Singh (virphfph@iitr.ernet.in)

finding of Hill et al. (2000) is that the rate coefficient for the reaction N_2 ($A^3\sum_u^+$) with O is temperature dependent. This new finding is very important as it has a major impact on earlier dayglow model results, in particular on the greenline dayglow emission.

Recently, Witasse et al. (1999) have modelled O(^{1}S) thermospheric dayglow at higher latitudes and higher solar zenith angles (76°−84°) using the TRANSCAR model. This model also underestimated the emission rate in the vicinity of the thermospheric peak in two out of the three cases they considered. For solar zenith angles greater than 70°, the thermospheric peak is found above 180 km, where the impact of the N_2 ($A^3\sum_u^+$) reaction is minimal. The authors suggest that the cause of the discrepancy above 180 km might be due to the underestimation of superthermal electron impact (photoelectron flux).

A key problem in the modelling of the dayglow is the appropriate use of solar EUV flux. These solar EUV fluxes are involved in direct and indirect processes of excitation of atmospheric species which result in the production of airglow emissions. Hinteregger et al. (1981) and Tobiska (1991) are the two respective models which provide the solar fluxes under different solar activity conditions. Though these models take into account the variation of solar activity, they have different scaling techniques. Consequently, both of these models provide quite different solar EUV fluxes. One should exercise more care in using the solar EUV flux models.

In this paper, we present a re-analysis of the greenline dayglow emission profiles between 120–250 km measured by WINDII on board the Upper Atmosphere Research Satellite (UARS) in light of the proposed temperature dependence of the rate coefficient for the reaction N_2 ($A^3\sum_u^+$) with O. The glow model is updated using the temperature dependent rate coefficient of the reaction N_2 ($A^3\sum_u^+$)+ O, and the volume emission rates (VER) of the greenline dayglow emission are calculated using the Hinteregger et al. (1981) and Tobiska (1991) solar EUV flux models.

2 Model

Mechanisms for the production of the O(^{1}S) dayglow emissions have been discussed by Tyagi and Singh (1998). In the lower thermosphere the four major sources for these emissions are the photoelectron impact excitation of atomic oxygen, dissociative recombination of O_2^+, energy transfer to atomic oxygen from N_2 ($A^3\sum_u^+$) and photodissociation of molecular oxygen. In the model calculations presented below, the same parameters as used by Tyagi and Singh (1998) are being used, with the exception that the temperature dependence of the rate coefficient of the reaction N_2 ($A^3\sum_u^+$)+ O, as proposed by Hill et al. (2000), is now included. The new rate coefficients for the $v' = 0$, 1 and 2 vibrational levels are $(3.4\pm0.8) \times 10^{-11}(T/298)^{0.5}$, $(5.6 \pm 1.3) \times 10 - 11$ $(T/298)^{0.5}$ and $(4.8 \pm 1.2)^{-11}(T/298)^{0.5}$, respectively. In the present calculations we have only used the rate coefficient for $v' = 0$, because for higher vibrational levels the branching ratio is not known. The branching ratio can only be known if the photoelectron impact excitation cross sections for the N_2 ($A^3\sum_u^+$) state are known separately for vibrational levels $v' = 0$, 1 and 2. Unfortunately, these individual cross sections are not available in the literature. However, the total photoelectron impact excitation cross section for the N_2 ($A^3\sum_u^+$) state is known, which includes all the possible vibrational levels. Consequently, we have assumed that the N_2 ($A^3\sum_u^+$) state is produced in the $v' = 0$ vibrational state. The density of N_2 ($A^3\sum_u^+$) for v′ = 0 level is obtained under a photochemical equilibrium condition. This assumption may be of some error. However, it was the conclusion of Hill et al. (2000) that the higher vibrational levels contribute less to the production of O(^{1}S), and this finding has been supported in the theoretical work of Kirillov (1997). It has been pointed out in the Introduction that the quantum yield of O(^{1}S) production due to the reaction of N_2 ($A^3\sum_u^+$) with O has been the subject of considerable discussion in recent years. Hill et al. (2000) have given a very detailed history of the quantum yield. The various values of the quantum yield, which range from 0.36 to 0.75, have been obtained using airglow and auroral studies by various workers (Frederick et al., 1976; DeSouza et al., 1985; Singh et al., 1996; Bucsela et al., 1998; Strickland et al., 2000). Hill et al. (2000) proposed a value of 0.47 ± 0.17 of the quantum yield for the reaction N_2 ($A^3\sum_u^+$)+ O. Consequently, we have used the values of 0.36, 0.47 and 0.75 for the quantum yield of O(^{1}S) production due to the reaction N_2 ($A^3\sum_u^+$)+ O, to obtain the O(^{1}S) emission profiles. These three values are used in the model to compare the O(^{1}S) emission rates with the WINDII observations and to find out the suitable value which would give better agreement with the WINDII measurements. The O(^{1}S) emission profiles are obtained using the production rates from the various sources discussed above and by taking into account the appropriate loss processes (Singh et al., 1996) under photochemical equilibrium conditions. The solar EUV flux plays a very important role in the production of dayglow emissions. The results are quite sensitive to the values of solar irradiance. Consequently, one should exercise care in using the solar EUV flux model. Hinteregger et al. (1981) and Tobiska (1991) are the two respective models which provide the solar EUV fluxes under different solar activity conditions. Though these models take into account the variation of solar activity, they have different scaling techniques. Consequently, both of these models provide quite different solar EUV fluxes. Therefore, it would be more appropriate to make use of both of these models in the calculations and to find out which model gives a better agreement with the measurements.

In the Hinteregger et al. (1981) model the solar EUV flux is scaled using a parameterization method based on daily 10.7 cm solar radio flux and its 81-day average flux. The reference solar spectrum is chosen from SC# 21 REF. For ionizing EUV, Hinteregger et al. (1981) have used a contrast ratio method which is based on the bin structure very similar to Torr and Torr (1985). The Lyman α and Fe XVI (335 Å) enhancement ratios are used to account for solar activity. The

following equations are used for the scaling of solar flux:

$$\mathrm{SFLUX} = [\mathrm{RFLUX} + \{(R_1 - 1)S_1 + (R_2 - 1) \times S_2\}/1000],$$

Where SFLUX is scaled solar Flux, and RFLUX is reference solar Flux. S_1 are scaling factosr for Fe (XVI) coronal emission (335 Å), R_1 = 1+ 0.0138 × (F10.7A–71.5) + 0.005 × (F10.7–F10.7A + 3.9), and R_2 = 1+ 0.59425 × (F10.7A–71.5) + 0.3811 × (F10.7–F10.7A + 3.9). There are 59 values for each S_1 and S_2, which corresponds to 59 bins of solar spectrum (the values of S_1 and S_2 are given in the subroutine SSFLUX of the glow model).

In the Tobiska (1991) model the solar EUV flux is scaled using a parameterization method based on the Lyman α slope for chromospheric fluxes and an He I 10830 Å equivalent width. This model also takes into account the daily 10.7 cm solar radio flux and its 81-day average flux. The following equations have been used by Tobiska (1991) for scaling the solar flux:

SFLUX = TCHRO + TCHR1 × HLYMOD + TCHR2 × HEIMOD + TCORO + TCOR1 × F10.7 + TCOR2 × F10.7A.

where

TCHRO = Intercept of chromospheric fluxes, EUV 91 model.
TCHR1 = H Lyman $\propto$ slope for chromospheric fluxes.
TCHR2 = He Fluxes 10 830 Å equivalent width slope for chromospheric fluxes.
TCOR0 = Intercept for coronal fluxes.
TCOR1 = F10.7 slope for coronal fluxes.
TCOR2 = F10.7A slope for coronal fluxes.
HLYMOD = HEIEW $\times 3.77847 \times 10^9 + 8.40317 \times 10^{10}$ (for HEIEW > 0.001).
HLYMOD = 8.70E8 × F10.7 + 1.90 $\times 10^{11}$ (for HEIEW $\leq$ 0.001).
HLYMOD = HLYA (for HLYA > 0.001).
HEIMOD = HEIEW $\times 3.77847 \times 10^9 + 8.40317 \times 10^{10}$ (for HEIEW > 0.001).
HEIMOD = HLYMOD (for HEIW $\leq$ 0.001).

where HEIEW = He I 10830 Å equivalent width HLYA = H Lyman $\propto$ flux. The values of the above parameters are listed in the subroutine SSFLUX of glow model.

3 Results and discussion

The 5577 Å dayglow volume emission rates (VER) are calculated at several latitudes and local times for which WINDII data is available in both hemispheres. For illustration purposes, we have chosen eight cases at various latitudes and local times in both hemispheres. The measured and modelled VER for these cases are shown in Figs. 1–5. The VER are calculated using Hinteregger et al. (1981) and Tobiska (1991) solar EUV flux models. In Fig. 1 we have shown the comparison between the emission profiles obtained using the quantum yield of 0.36 and 0.75, along with WINDII

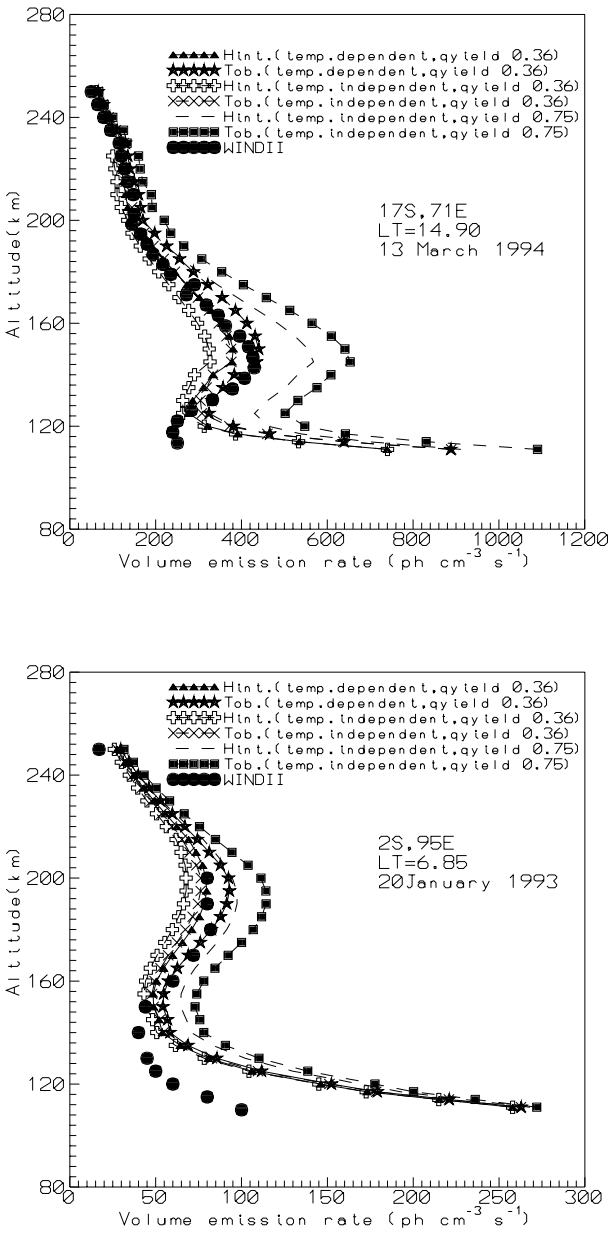

Fig. 1. Comparison between the observed and modelled O(^{1}S) VER profiles. The darkened triangles and darkened asterisks are for the Hinteregger et al. (1981) and Tobiska (1991) solar EUV flux models with the temperature dependent rate coefficient of reaction N_2 ($A^3\sum_u^+$)+ O and a quantum yield of 0.36. The plus and the multiplication signs are for the Hinteregger et al. (1981) and Tobiska (1991) solar EUV flux models with the temperature independent rate coefficient of reaction N_2 ($A^3\sum_u^+$)+ O and a quantum yield of 0.36. The dashed line and the darkened squares are for the Hinteregger et al. (1981) and Tobiska (1991) solar EUV flux models with the temperature independent rate coefficient of reaction N_2 ($A^3\sum_u^+$)+ O and a quantum yield of 0.75. The darkened circles are the observed VER from WINDII.

observations for both the solar EUV flux models. It is quite clear from the profiles shown in Fig. 1 that the results ob-

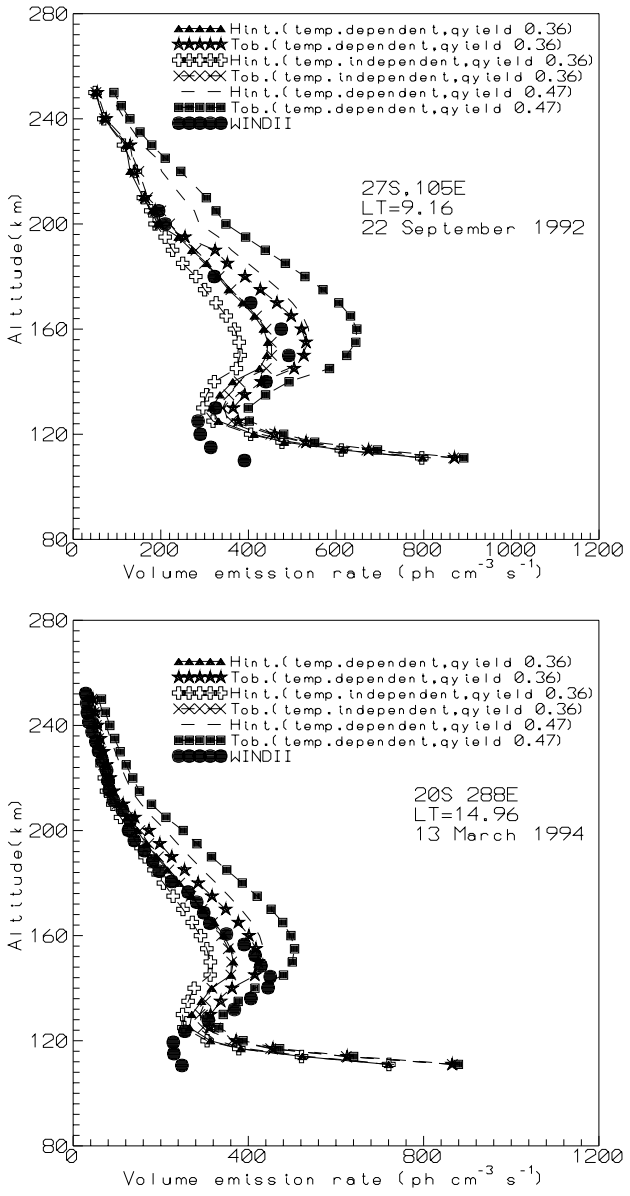

Fig. 2. Comparison between the observed and modelled O(^{1}S) VER profiles. The darkened triangles and darkened asterisks are for the Hinteregger et al. (1981) and Tobiska (1991) solar EUV flux models with the temperature dependent rate coefficient of reaction N_2 ($A^3\sum_u^+$)+ O and a quantum yield of 0.36. The plus and the multiplication signs are for the Hinteregger et al. (1981) and Tobiska (1991) solar EUV flux models with the temperature independent rate coefficient of N_2 ($A^3\sum_u^+$)+ O and a quantum yield of 0.36. The dashed line and the darkened squares are for the Hinteregger et al. (1981) and Tobiska (1991) solar EUV flux models with the temperature dependent rate coefficient of reaction N_2 ($A^3\sum_u^+$)+ O and a quantum yield of 0.47. The darkened circles are the observed VER from WINDII.

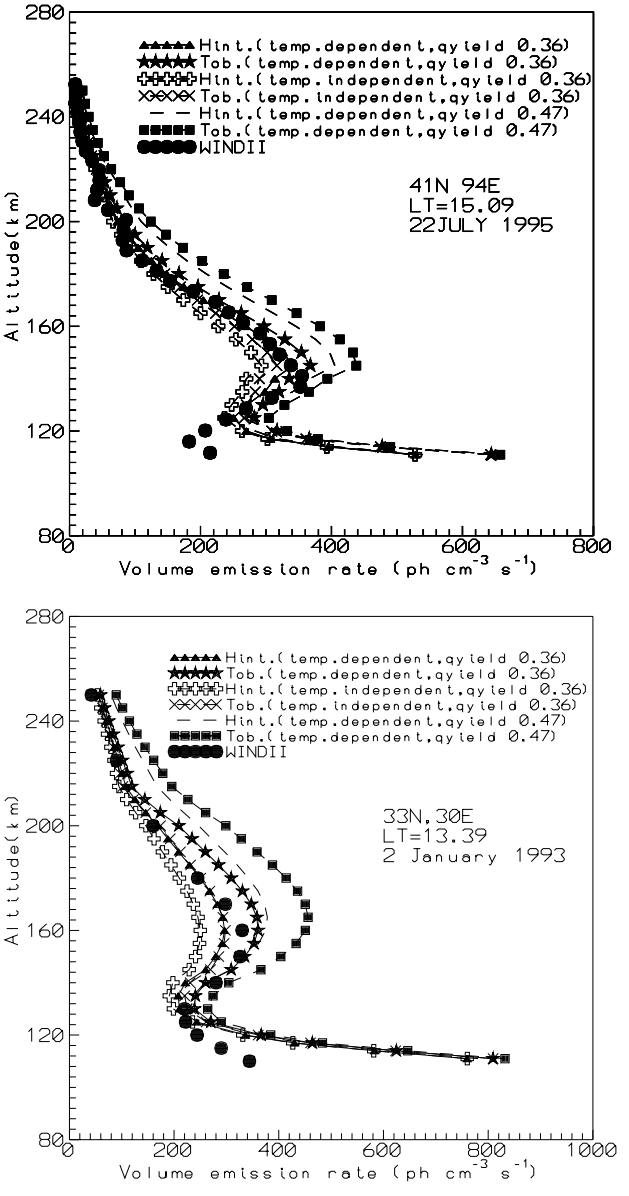

Fig. 3. Same as in Fig. 2 but at different latitudes and local times.

tained using the temperature dependent rate coefficient (Hill et al., 2000) and the Hinteregger et al. (1981) solar EUV flux model (with quantum yield 0.36) are in very good agreement with the WINDII observations, and they reproduce the thermospheric peak as observed from WINDII within an error of 8%. It is also quite clear from the Fig. 1 that the VER labelled as Hint. (temp. independent, qyield 0.36), obtained using Hinteregger et al. (1981) solar EUV flux model with temperature independent rate coefficient (Piper et al., 1981), are significantly smaller than the measured emission rates in the thermospheric peak region. Further, it is noticeable from Fig. 1 that the emission profiles obtained using the quantum yield of 0.75, along with the temperature independent rate coefficient taken from the Piper et al. (1981), are significantly higher than the WINDII observations for both the solar EUV flux models. These results indicate that the quantum yield of 0.75, which was proposed by Piper et al. (1981), is not suitable to explain the WINDII observations.

In Figs. 2 and 3 we have shown the comparison between

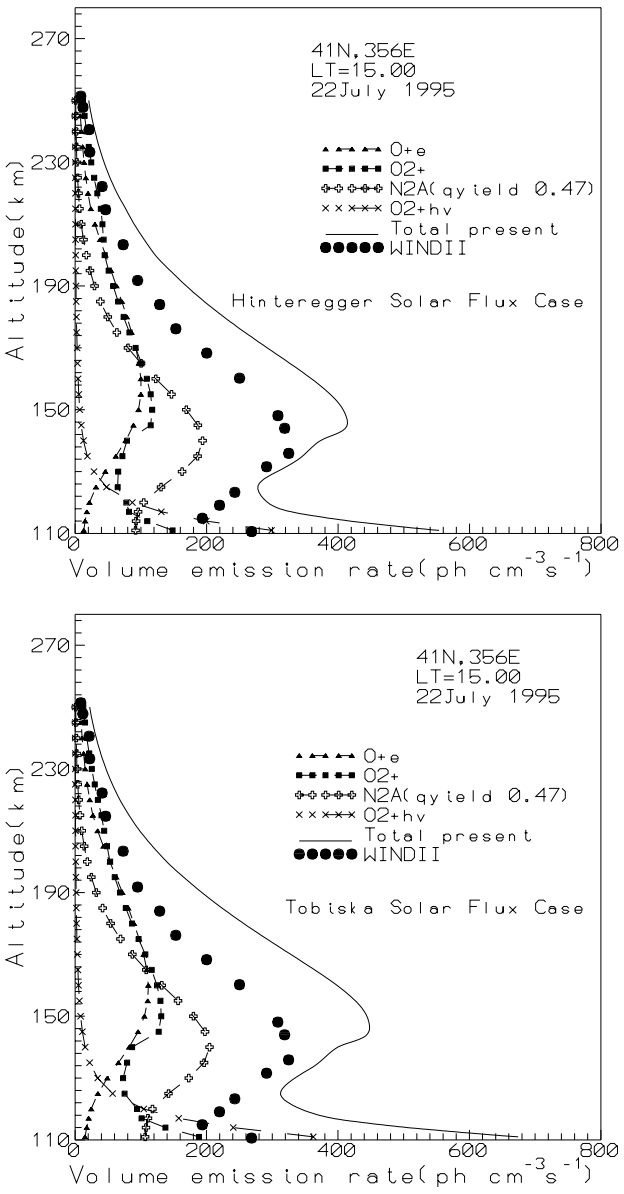

Fig. 4. Modelled and measured greenline dayglow emission profiles for selected observing (WINDII) conditions along with the various contributions of the O(^{1}S) production processes.

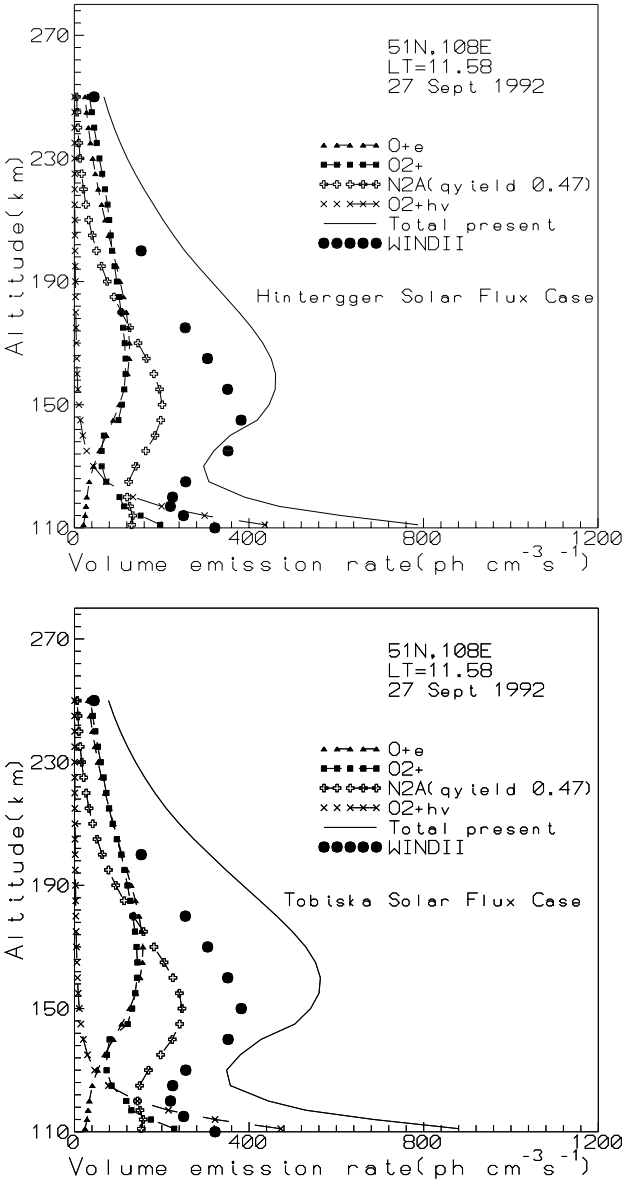

Fig. 5. Same as in Fig. 4. but at different latitudes and local times.

the emission profiles obtained using the quantum yield of 0.36 and 0.47 (Hill et al., 2000). It is quite evident from Figs. 2 and 3 that the results obtained using the temperature dependent rate coefficient (Hill et al., 2000) and the Hinteregger et al. (1981) solar EUV flux model (with quantum yield 0.36) are in very good agreement with the WINDII observations, and they reproduce the thermospheric peak as observed from WINDII within an error of 8%. It is also quite evident from Figs. 2 and 3 that the emission profiles obtained using the quantum yield of 0.47, as proposed by Hill et al. (2000), are about 20% and 40% higher than the WINDII observations for Hinteregger et al. (1981) and Tobiska (1991) solar EUV flux models, respectively, in the thermospheric peak region.

The individual components of O(^{1}S) production due to various sources are shown in Figs. 4 and 5 for both solar EUV flux models. Two representative cases, one at local noontime and other in the afternoon, have been chosen. A value of 0.47 is used for the quantum yield of reaction N_2 ($A^3\sum_u^+$) with O. It is noticeable from these figures that the reaction of N_2 ($A^3\sum_u^+$) with O is the dominating source of O(^{1}S) between 130 and 170 km. In the earlier studies of Singh et al. (1996) and Tyagi and Singh (1998), which were based on the temperature independent rate coefficient of the reaction N_2 ($A^3\sum_u^+$)+ O and a quantum yield of 0.36, the contribution of this reaction was comparable with that of the dissociative recombination reaction O_2^+ + e between 130 and 170 km. Further, it is quite evident from Figs. 4 and 5 that the photodissociation of O_2 becomes the major source of O(^{1}S)

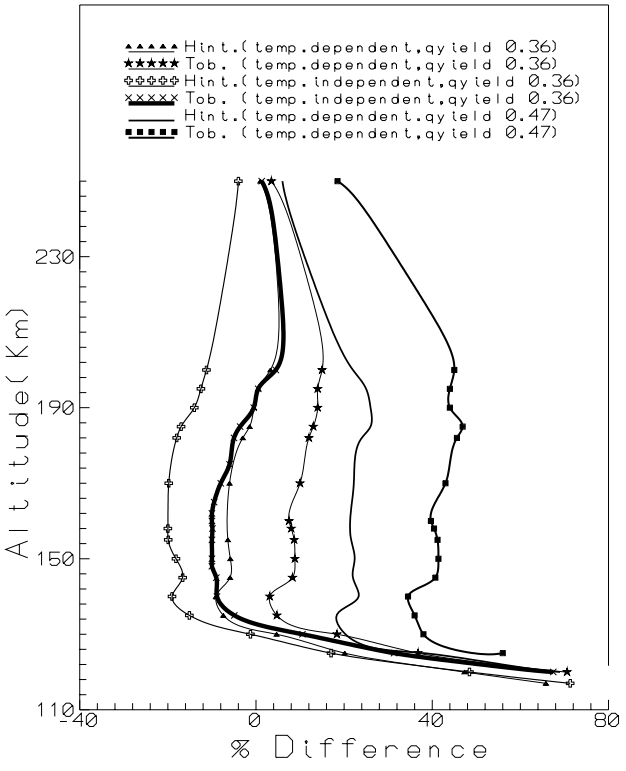

Fig. 6. The mean % difference in the VER between the observations (WINDII) and modelled results. The darkened triangles and darkened asterisks are for the Hinteregger et al. (1981) and Tobiska (1991) solar EUV flux models with the temperature dependent rate coefficient of reaction N_2 ($A^3\sum_u^+$)+ O and a quantum yield of 0.36. The plus and the multiplication signs are for the Hinteregger et al. (1981) and Tobiska (1991) solar EUV flux models with the temperature independent rate coefficient of reaction N_2 ($A^3\sum_u^+$)+ O and a quantum yield of 0.36. The dashed line and the darkened squares are for the Hinteregger et al. (1981) and Tobiska (1991) solar EUV flux models with the temperature dependent rate coefficient of reaction N_2 ($A^3\sum_u^+$)+ O and a quantum yield of 0.47.

below 120 km. The O(^{1}S) emission profiles obtained in the present model are significantly higher than the WINDII observations below 120 km. The main problem for this discrepancy arises from the scaling of solar fluxes between 900 Å and 1350 Å. This problem can only be resolved if the simultaneous measurements of solar flux are available for the day on which measurements have been taken for O(^{1}S) dayglow emission.

Further, it is quite evident from Figs. 1–3 that the emission rates obtained using the Tobiska (1991) solar EUV flux model (with quantum yield 0.36) and the temperature independent reaction rate coefficient of N_2 ($A^3\sum_u^+$)+ O are also in good agreement (with in 10%) with the measured emission rates, whereas the emission rates obtained with the temperature dependent rate coefficient are marginally higher (about 12%) than the measured emission rates. One may also notice that the emission rates obtained from the Tobiska (1991) solar EUV flux model are about 20–30% higher than those emission rates obtained from the Hinteregger et al. (1981) solar EUV flux model in all the corresponding cases. The main reason of this difference is due to the fact that the Tobiska flux model provides about 20–30% higher values of EUV flux than that of the Hinteregger et al. (1981) solar EUV flux model below the 300 Å wavelength. The energy associated with solar radiation below 300 Å is responsible mainly for the production of greenline dayglow emission in the thermosphere (above 120 km). Consequently, the Tobiska (1991) solar EUV flux model would provide higher values of emission rates than those obtained from the Hinteregger et al. (1981) solar EUV flux model.

The mean percentage difference of the unrevised and the revised results with the WINDII results are shown in Fig. 6, for both the solar EUV flux models. The mean VER is obtained from the analysis of several greenline dayglow profiles (twenty in numbers) at various latitudes and local times in both hemispheres. The percentage difference between the modelled and WINDII results is calculated at a particular altitude for each profile. After obtaining the percentage difference at a particular altitude, the simple average is obtained for all the emission profiles. One can notice from Fig. 6 that the revised results obtained from the Hinteregger et al. (1981) solar EUV flux model are within 8% agreement with the WINDII results between 120 and 200 km, which shows significant improvement over the corresponding unrevised results. In case of the Tobiska (1991) solar EUV flux model, the VER with the temperature independent rate coefficient are 10% smaller than the WINDII results between 120 to 200 km. It is also evident from Fig. 6 that the VER obtained with the temperature dependent rate coefficient in the Tobiska (1991) solar EUV flux model are about 12% higher than the WINDII results between 120 and 200 km. One can also notice in Fig. 6 that the VER obtained using a quantum yield of 0.47 with the temperature dependent rate coefficient are about 20% and 40% higher than the WINDII results for the Hintergger et al. (1981) and Tobsika (1991) solar EUV flux models, respectively, in the thermospheric peak region (120–200 km).

The following points have emerged from the above discussion:

1. The VER obtained using the Hinteregger et al. (1981) solar EUV flux model, along with the temperature dependent rate coefficient and a quantum yield of 0.36 for the reaction N_2 ($A^3\sum_u^+$)+ O, are in very good agreement with the WINDII results in the thermospheric peak region.

2. The VER obtained using the Tobiska (1991) solar EUV flux model, along with the temperature dependent rate coefficient and a quantum yield of 0.36 for the reaction N_2 ($A^3\sum_u^+$)+ O, are about 12% higher than the WINDII results in the thermospheric peak region.

3. The VER obtained using the temperature dependent rate coefficient and a quantum yield of 0.47 are about 20%

and 40% higher than the WINDII results for the Hintergger et al. (1981) and Tobsika (1991) solar EUV flux models, respectively, in the thermospheric peak region.

4 Conclusions

The temperature dependence of the rate coefficient of reaction N_2 ($A^3\sum_u^+$)+ O proposed by Hill et al. (2000) has been incorporated in the glow model. The VER profiles are obtained using the Hinteregger et al. (1981) and the Tobsika (1991) solar EUV flux models. A comparative study of VER has been done at various latitudes and local times in both hemispheres. This study reveals that the emission profiles obtained using the Hinteregger et al. (1981) solar EUV flux model, along with the temperature dependent rate coefficient and a quantum yield of 0.36 for the reaction N_2 ($A^3\sum_u^+$)+ O, reproduce the thermospheric peak (within 8%) as observed by WINDII. These findings support the newly discovered temperature dependence of the rate coefficient of reaction N_2 ($A^3\sum_u^+$) with O. However, based on the discussion as given above in the text, it is extremely difficult to have any firm conclusion regarding the temperature dependence of rate coefficient of the reaction N_2 ($A^3\sum_u^+$)+ O in the case of the Tobiska (1991) solar EUV flux model.

Acknowledgements. The authors thank G. G. Shepherd and I. C. McDade, York University, Canada for providing the WINDII data. One of us (AKU) thanks I.S.R.O. Banglore for the financial support. This work is financially supported by the RESPOND programme of I.S.R.O.

Topical Editor D. Murtagh thanks T. Slanger and D. Gattinger for their help in evaluating this paper.

References

Akmaev, R. A. and Shved, G. M.: Modelling of the composition of the lower thermosphere taking accounts of the dynamics with application of tidal variation of the (OI) 5577Å airglow, J. Atmos. Terr. Phys., 42, 705, 1980.

Bates, D. R.: Oxygen green and red line emission and O_2^+ dissociative recombination, Planet. Space Sci., 38, 889, 1992.

Bucsela, E. J., Dymond, K. F., McCoy, R. P., and Cleary, D. D.: Atomic and molecular emissions in the MUV dayglow, J. Geophys. Res., 103, 29 215, 1998.

DeSouza, A. R., Gousset, G., Touzeau, M., and Kheit, T.: Note on the determination of the efficiency of the reaction N_2 ($A^3\sum_u^+$) + O(^{3}P) → N_2 + O(^{1}S), J. Phys. B At. Mol. Phys., 18, L661, 1985.

Feldman, P. D., Doering, J. P., and Zipf, E. C.: Excitation of O(^{1}S) atoms in the day airglow, J. Geophys. Res., 76, 3087, 1971.

Frederick J. E., Rusch, D. W., Victor, G. A., Sharp,W. E., Haya, P. B., and Brinton, H. C.: The OI (15500 Å) airglow: observations and excitation mechanism, J. Geophys. Res., 81, 3923, 1976.

Hinteregger, H. E., Fukui, K., and Gilson, B. R.: Observational references and model data on solar EUV from measurements on AE-E, Geophys. Res. Lett., 8, 1147, 1981.

Hill, S. M.,Solomon, S. C., Cleary, D. D., and Broadfoot, A. L.: Temperature dependence of the reaction N_2 ($A^3\sum_u^+$) + O in the terrestrial thermosphere, J. Geophys. Res., 105, 10 615, 2000.

Kirillov, A.: Application of Landau-Zener approximation in the calculation of rate coefficients of reaction N_2 ($A^3\sum_u^+$) + O(^{3}P)→ N_2($X^1\sum_g^+$) + O(^{3}P, ^{1}D, ^{1}S), paper presented at the 24th Annual European Meeting on Atmospheric studies by Optical methods, Andenes, Norway, 1997.

Piper, L. G., Caledonia, G. E., and Kennealy, J. P.: Rate constants for deactivation of N_2 ($A^3\sum_u^+$), v′= 0,1) by O, J. Chem. Phys., 75, 2847,1981.

Shepherd, G. G, Thuiller, G., and Gault, W. A. et al.: WINDII, the Wind Imaging Interferometer on the Upper Atmosphere Research Satellite, J. Geophys. Res., 98, 10 725, 1993.

Strickland, D. J., Hecht, J. H., Christensen, A. B., and McEwen, D. J.: Thermospheric disturbance recorded by photometers onboard the ARIA II rocket, J. Geophys. Res., 105, 2461, 2000.

Singh, V., Mcdade, I. C., Shepherd, G. G., Solheim, B. H., and Ward, W. E.: The O(^{1}S) dayglow emissions as observed by the WIND imaging interferometer on the UARS, Ann. Geophysicae, 14, 637, 1996.

Singh, V. and Tyagi, S.: Study of O(^{1}S) dayglow emission near equatorial latitude, Indian J. Radio Space Phys., 26, 36, 1997.

Tobiska, W. K.: Revised solar extreme ultraviolet flux model, J. Atmos. Terr. Phys., 53, 1005, 1991.

Torr, M. R. and Torr, D. G.: Ionization frequences for solar cycle 21, revised, J. Geophys. Res., 90, 665, 1985.

Torr, D. G., Torr, M. R., and Richard, P. G.: Thermospheric airglow emissions: A comparision of measurements from Atlas I and theory, Geophys. Res. Let., 20, 519, 1993.

Tyagi, S. and Vir Singh: The morphology of oxygen green line dayglow emission, Ann. Geophysicae, 16, 1599, 1998.

Wallace, L. and McElroy, M. B.: The visual dayglow, Planet Space Sci., 14, 667, 1966.

Witasse, O., Lilensten, J., Lathuilere, C., and Blelly, P. L.: Modeling the OI630.0 and 557.7 nm thermospheric dayglow during EISCAT-WINDII coordinated measurements, J. Geophys. Res., 104, 24 639, 1999.